Electronic Supplementary Material (ESI) for ChemComm.

SUPPORTING INFORMATION

Cucurbit[6]uril is an ultrasensitive ^{129}Xe NMR contrast agent

Yanfei Wang and Ivan J. Dmochowski

Department of Chemistry, University of Pennsylvania, 231 South 34th St., Philadelphia, PA 19104, USA

Table of Contents

1. Materials

All phosphate-buffered saline (PBS) used in this work was 1.058 mM potassium phosphate monobasic, 154 mM sodium chloride, and 5.6 mM sodium phosphate dibasic, pH 7.2.

The following organic and biological reagents were purchased from Sigma-Aldrich: Cucurbit[6]uril (CB[6]), putrescine (analytical standard), and plasma (from human).

2. Hyperpolarized ^{129}Xe NMR Spectroscopy

HP ^{129}Xe was generated using spin-exchange optical pumping (SEOP) method with a home-built ^{129}Xe hyperpolarizer, based on the commercial model IGI.Xe.2000 by GE. A gas mixture of 10% nitrogen, 89% helium, and 1% natural abundance xenon (Linde Group, NJ) was used as the hyperpolarizer input. 795 nm circularly polarized diode laser was used for optical pumping of Rb vapor.

^{129}Xe HP was hyperpolarized to 10–15% after being cryogenically separated, accumulated, thawed, and collected in controlled atmosphere valve NMR tubes (New Era). After Xe collection, 5 mm NMR tubes were shaken vigorously to mix solutions with Xe. Direct HP ^{129}Xe NMR measurements were performed on a Bruker BioDRX 500 MHz NMR spectrometer (138.12 MHz frequency for ^{129}Xe), using a 5-mm BBO NMR probe. Sample temperature was controlled by VT unit on NMR spectrometer to 300 ± 1 K. Spectrum was collected 30-60 seconds after sample insertion. Chemical shifts were referenced relative to ^{129}Xe gas at 0 ppm when extrapolated to 0 atm.

3. Hyper-CEST Experiments

Prior to applying saturation pulse, a controllable amount of HP ^{129}Xe was delivered into a 2.5 mL sample solution and sealed in the NMR tube by a home-built continuous-flow gas delivery setup. For each data point in the Hyper-CEST spectrum, the gas mixture was bubbled for 20 seconds, followed by a 3-second delay to allow bubbles to collapse. All Hyper-CEST experiments were carried out using a Bruker 500 MHz NMR spectrometer, with 10-mm PABBO probe. A 90° hard pulse of this probe has pulse length of 22 μs.

3.1 For Hyper-CEST frequency-scan profile (Figure 2 and Figure 4), saturation pulse Dsnob with 690 Hz bandwidth was used. Pulse length t_{pulse} = 3.80 ms, field strength $B_{1,max}$ = 77 μT, number of pulses n_{pulse}= 400, saturation time t_{sat} = 1.52 s.

3.2 For saturation time curves (Figure 3 and Figure S3), saturation pulse Dsnob with 2500 Hz bandwidth was used. Pulse length t_{pulse} = 1.05 ms, field strength $B_{1,max}$ = 279 μT, number of pulses linearly increased from 0 to 6000, saturation time t_{sat} correspondingly increased from 0 to 6.3 sec. Figures were fitted with mono-exponential decay function y = exp (-x/τ).

3.3 For Table 1 and Figure S5, saturation pulse Dsnob with 833 Hz bandwidth was used. Pulse length t_{pulse} = 3.15 ms, field strength $B_{1,max}$ = 92 μT, number of pulses linearly increased from 0 to 2000, saturation time t_{sat} correspondingly increased from 0 to 6.3 sec. The calculation of *ST* efficiency was based on the equation below, where I represents the acquired post saturation Xe(aq) signal with set saturation frequency, duration, and power. L represents the duration of Hyper-CEST pulse sequences. The index *k* indicates the experiment number in Figure S5.

$$ST = \sum_{k} \frac{I_{off}^{k} - I_{on}^{k}}{I_{off}^{k}} \frac{L^{k}}{\sum_{k'} L^{k'}}$$

4. Hyperpolarized ^{129}Xe Exchange Spectroscopy

HP gas was directly bubbled into the 3-mL sample solution through capillaries for 20 sec (flow rate 0.7 L per min), followed by a 2-sec delay to allow bubbles to collapse. Subsequently three successive 90 degree pulses were applied. The above process was repeated for each point in the t1 domain. And the following equations were used to evaluate rate constants.

$A = \exp\left(-R\tau_m\right)$,(1) $\qquad A = \begin{vmatrix} I_{11}/M_1 & I_{12}/M_2 \\ I_{21}/M_1 & I_{22}/M_2 \end{vmatrix}$

$R = \frac{-X\,(\ln D)X^{-1}}{\tau_m}$, $R = \begin{vmatrix} -R_1 - k_1^{'} & k_{-1}^{'} \\ k_1^{'} & -R_2 - k_{-1}^{'} \end{vmatrix}$

A is a matrix which contains the peak amplitudes measured at a certain mixing time τ_m divided by the intensities of the diagonal peaks in the reference spectrum (0 mixing time). Matrix R is the solution to equation 1, according to eigenvector method, and it contains the kinetic parameters to be determined, $k_1^{'}$ *and* $k_{-1}^{'}$ (k_{on} and k_{off}).

5. Hyper-CEST Efficiency for Different Concentrations of Putrescine

By fitting Hyper-CEST signal to an exponential decay function[1] (Figure S5), we extracted the decay constants for both on-resonance (122.3 ppm = 193.5 – 71.2 ppm)) and off-resonance (264.7 ppm = 193.5 + 71.2 ppm) for each sample. Using the first-order kinetics approximation, the difference of on- and off-resonance relaxation rate was hypothesized to be a linear function of the concentration of available exchange sites (i.e., free CB[6]). Such fitting provided an empirical estimation of parameter ***p*** in Equation **4**, in which other coefficients and constants including relaxation rate, exchange kinetics and field strength were incorporated.

$$K_A = \frac{c_{CB[6]bound}}{(c_{putr} - c_{CB[6]bound}) * (c_{CB[6]} - c_{CB[6]bound})} \quad (1)$$

Equation (1) is equivalent to

$$K_A = \frac{c_{CB[6]} - c_{CB[6]free}}{(c_{putr} + c_{CB[6]free} - c_{CB[6]}) * c_{CB[6]free}} \quad (2)$$

where $\boldsymbol{c_{CB[6]bound}}$ is the putrescine-bound CB[6] concentration, $\boldsymbol{c_{CB[6]free}}$ is the free CB[6] concentration, $\boldsymbol{c_{CB[6]}}$ is the total CB[6] concentration and $\boldsymbol{c_{putr}}$ is the putrescine concentration. Using the first-order kinetics approximation, the difference of on- and off-resonance relaxation rate (λ_{on} - λ_{off}) was hypothesized to be a linear function of the concentration of available CB[6] exchange sites ($c_{CB[6]free}$).

Hence, we have

$$c_{CB[6]free} = p * \lambda_{diff} = p * (\lambda_{on} - \lambda_{off}) \quad (3)$$

where *p* incorporates other coefficients and constants including spin-spin relaxation rate and field strength.

$$c_{putr} = \frac{c_{CB[6]} - p * \lambda_{diff}}{K_A * p * \lambda_{diff}} + c_{CB[6]} - p * \lambda_{diff} \quad (4)$$

where $\mathbf{c_{CB[6]}}$ is the concentration of CB[6] (1 μM), $\boldsymbol{K_A}$ is the association constant for putrescine binding to CB[6], $\boldsymbol{\lambda_{diff}}$ is the difference of on- and off-resonance decay rate derived from Hyper-CEST experiment, $\boldsymbol{c_{putr}}$ is the putrescine concentration. Data fitting (Figure S**6**) the experimentally determined $\boldsymbol{\lambda_{diff}}$ values for the biologically relevant range of putrescine concentrations gave a *p* value that was in good agreement with the theoretically predicted *p* value.

Equation 4 is used for curve fitting in Figure S6.

As Zaiss et al. discussed,[1]

$$\lambda_{diff} = \frac{k_a}{1 + k_b * (k_b + R_{2b})/w_1^2}, \quad where\ k_a = \frac{M_b}{M_a} * k_b \quad (5)$$

As $w_1 >> k_b^2 + k_b * R_{2b}$ in these experiments, the above could be simplified as,

$$\lambda_{diff} = \frac{M_b}{M_a} * k_b = k_b * K_A * c_{CB[6]free} = k_b * K_A * p * \lambda_{diff} \quad (6)$$

From above *p* is estimated to be 1/ (840 s^{-1} * 490 M^{-1}) = 2.4*10^{-6} M*s, which is similar to the fitted value (Figure S6).

Figures:

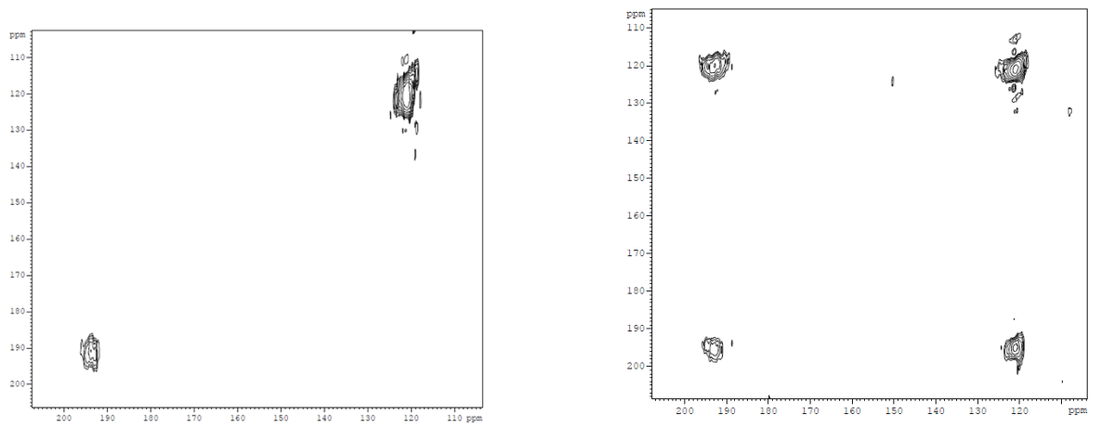

Figure S1. 2D HP ^{129}Xe EXSY spectra in the presence of 5 mM CB[6] in PBS with 0 s mixing time (control, left) or 2 ms mixing time (right).

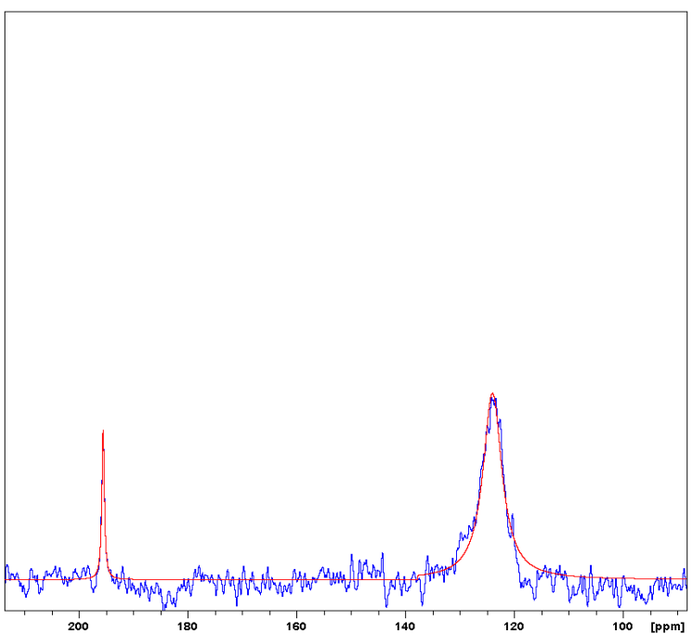

Figure S2. HP ^{129}Xe NMR spectrum of 0.5 mM cucurbit[6]uril in PBS, pH 7.2, 300 K. Eburp2-shaped pulses (2000 Hz width) were used to selectively excite Xe@CB[6] peak. A delay of 0.5 s was given between scans to allow for Xe exchange from solution into CB[6]. Spectra were averaged over 4 scans. Fourier-transformed spectra were processed with zero filling and Lorentzian line-broadening of 50 Hz. The Xe-CB[6] peak width (FWHM) is 470 Hz (magnetic homogeneity corrected), which corresponds to k_{off} of 1470 s^{-1}.

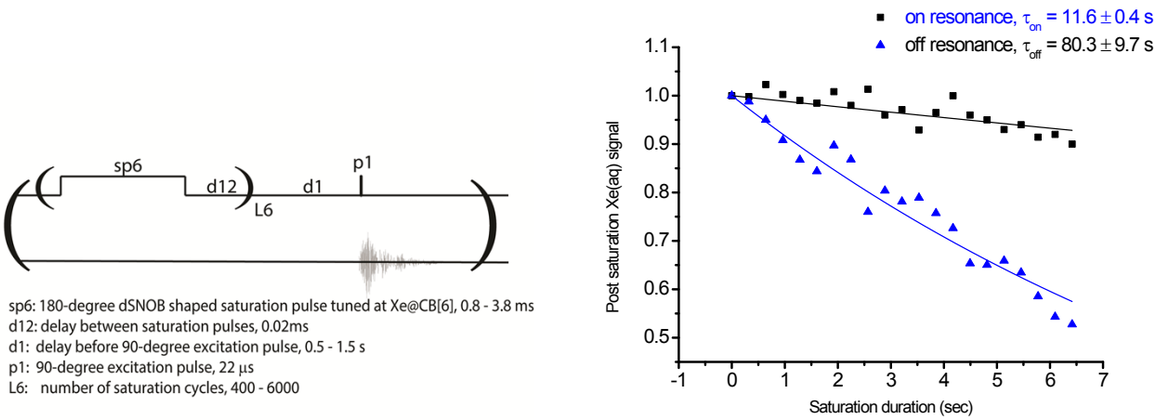

Figure S3. Left: Hyper-CEST pulse sequence diagram, with parameters used for in-house 10-mm PABBO probe. Different values were used for different sample concentration and HP Xe flow rate, to realize high sensitivity or resolution. Right: An example of Hyper-CEST profile of 18 pM CB[6] in pH 7.2 PBS at 300 K. Saturation frequencies of Dsnob-shaped pulses were positioned at 122.3 = (193.5 – 71.2) ppm and 264.7 = (193.5 + 71.2) ppm, for on- and off-resonance.

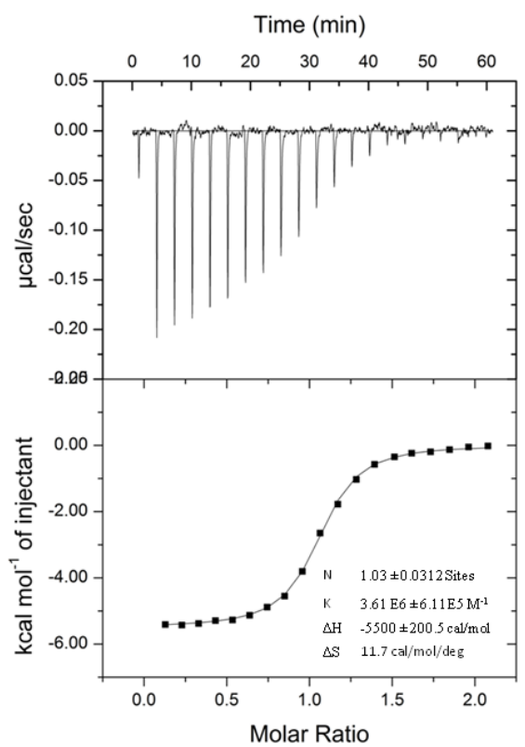

Figure S4. ITC measurements performed with CB[6] at 300 K. 200 µM putrescine was titrated into 20 µM CB[6].

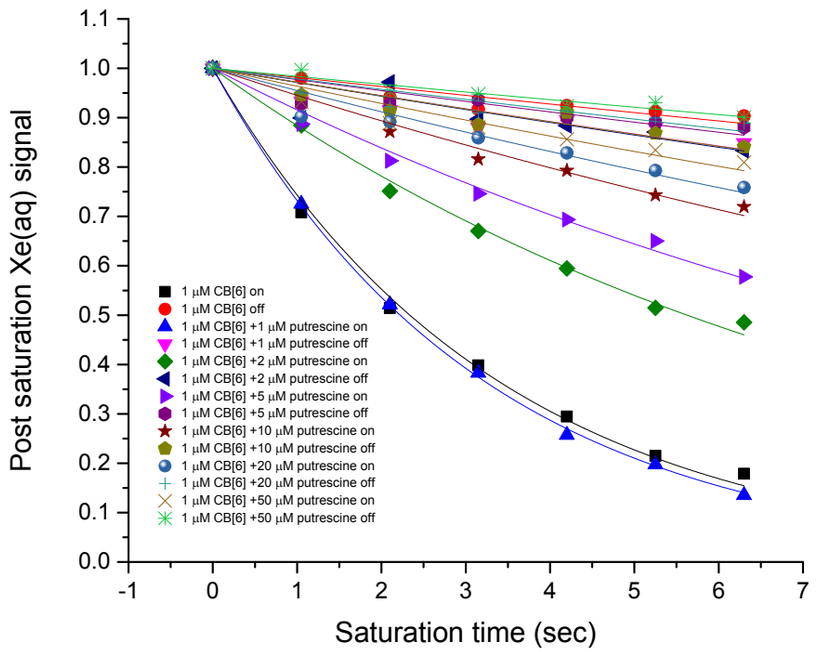

Figure S5. Hyper-CEST profiles of 7 different samples in pH 7.2 PBS buffer at 300 K. Saturation frequencies of Dsnob-shaped pulses were positioned at 122.3 = (193.5 – 71.2) ppm and 264.7 = (193.5 + 71.2) ppm, for on- and off-resonance. Data were fit with mono-exponential decay function y = exp (-x/t1).

Table S1. Fitting statistics for Figure S5. t1 is the exponential decay time constant, k = 1/t1 is the decay rate, tau = t1 * ln 2 is the mean lifetime.

	y0	**A1**	**t1**	**t1**	**k**	**k**	**tau**	**Statistics**	**Statistics**
	Value	Value	Value	Standard Error	Value	std err	Value	Reduced Chi-Sqr	Adj. R-Square
1 μM CB[6] on	0	1	3.37176	0.07358	0.29658	0.006472	2.33712	2.94E-04	0.99664
1 μM CB[6] off	0	1	53.24035	4.60424	0.01878	0.001624	36.9034	2.19E-04	0.83776
1 μM CB[6] +1 μM putrescine on	0	1	3.20652	0.02856	0.31186	0.002777	2.22259	4.83E-05	0.99951
1 μM CB[6] +1 μM putrescine off	0	1	35.04003	3.59041	0.02854	0.002920	24.2879	6.43E-04	0.73133
1 μM CB[6] +2 μM putrescine on	0	1	8.11589	0.17207	0.12322	0.002612	5.62551	2.07E-04	0.99434
1 μM CB[6] +2 μM putrescine off	0	1	34.44633	4.46034	0.02903	0.003758	23.87638	1.06E-03	0.68633
1 μM CB[6] +5 μM putrescine on	0	1	11.36809	0.31507	0.08797	0.002438	7.87976	2.50E-04	0.98809
1 μM CB[6] +5 μM putrescine off	0	1	43.28092	4.92099	0.0231	0.002626	30.00005	5.48E-04	0.65595

1 µM CB[6] +10 µM putrescine on	0	1	17.78367	0.56703	0.05623	0.001792	12.3267	1.84E-04	0.9829
1 µM CB[6] +10 µM putrescine off	0	1	34.91285	3.03295	0.02864	0.002488	24.19974	4.65E-04	0.83062
1 µM CB[6] +20 µM putrescine on	0	1	21.69607	1.33518	0.04609	0.002836	15.03857	5.09E-04	0.91999
1 µM CB[6] +20 µM putrescine off	0	1	46.04456	5.174	0.02172	0.002440	31.91566	4.80E-04	0.65711
1 µM CB[6] +50 µM putrescine on	0	1	27.10952	1.87783	0.02689	0.002555	18.79089	4.52E-04	0.88971
1 µM CB[6] +50 µM putrescine off	0	1	60.95673	4.11003	0.01641	0.001106	42.25199	1.04E-04	0.92448

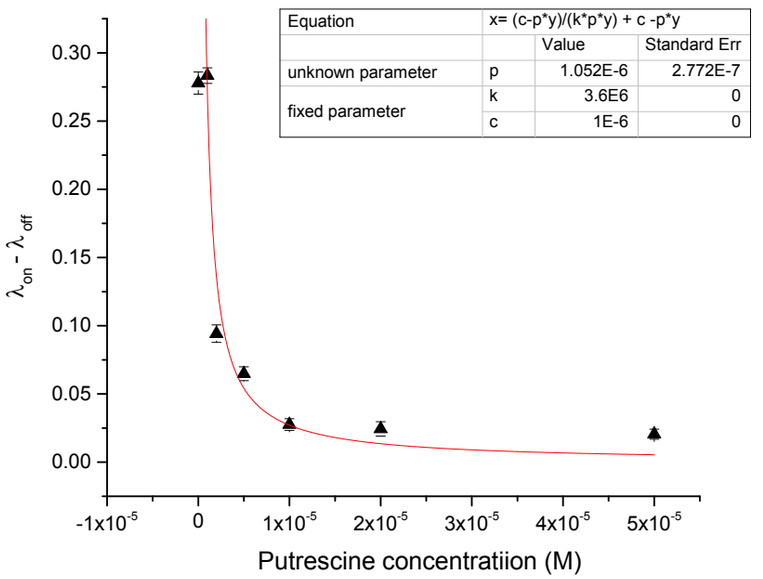

Figure S6. Decay rate difference plotted as a function of putrescine concentration.

Reference

1. M. Zaiss, M. Schnurr and P. Bachert, *J. Chem. Phys.*, 2012, **136**, 144106.